Measurement of U I and U II relative oscillator strengths*

Paul A. Voigt
National Bureau of Standards, Institute for Basic Standards, Washington, D. C. 20234
(Received 10 February 1975)

Relative *gf* values for 49 prominent U II lines and 21 of the strongest U I lines have been measured. The U II measurements were made using a wall-stabilized arc into which the uranium was introduced in the form of UF_6. The U I values were measured with a flow-stabilized arc which is essentially a free-burning arc stabilized by streaming argon around one of the electrodes which is formed from a molten ball of uranium held in a tungsten cup. Temperatures in the wall-stabilized and flow-stabilized arc were 10 500 K and 5500 K, respectively. The U I relative *gf* values were placed on an absolute scale employing a recent lifetime determination for the 27 887-cm^{-1} level of U I. This absolute scale was extended to the U II values by measuring the relative intensity of a U I and a U II line in the wall-stabilized arc.

INTRODUCTION

This work describes the experimental determination of relative *gf* values for atomic and singly ionized uranium. Uranium presents a special problem because of the complexity of its spectrum. It is estimated that over 300 000 lines of U I and U II can be observed and measured with modern high-resolution apparatus. Current measurements[1] in the wavelength region of this experiment (2900–5500 Å) indicate that the spectral line density is approximately 25 lines/Å. With the resolution obtained in this experiment (at best 0.05 Å), only the stronger uranium lines could be measured. Even for the stronger lines, careful checking was necessary to ascertain whether blending with weaker lines was negligible.

Two different arc sources were used in the experiment, and they will be referred to throughout as the flow-stabilized arc and the wall-stabilized arc. The flow-stabilized arc is essentially a free burning arc, which runs stably at a much lower axis temperature than the wall-stabilized arc (5500 K as compared to 10 500 K when burning with uranium) and was used for the measurement of U I lines. This type of arc was first used by Richter and Wulff[2] in the measurement of Fe I lines. Because of the very low ionization potential of uranium (6.22 eV), only a few of the strongest U I lines were observable in the higher-temperature wall-stabilized arc, and the U II spectrum remained stronger, even in the flow-stabilized arc. The flow-stabilized arc is viewed side-on between the electrodes, and since the observed intensity is integrated over zones of different temperature, an Abel inversion process must be used to obtain local intensity and temperature values. The principal advantage of the flow-stabilized arc is that low-temperature plasma conditions are achieved where the metal lines are quite intense, and there is very little continuum radiation; hence, many weaker lines can be measured. Disadvantages are that the electron density cannot be accurately determined and also is too low to guarantee complete local thermal equilibrium (LTE). The wall-stabilized arc operates in a stable fashion only at a higher temperature and electron density and can be viewed end-on through the electrodes. The arc is typically run in argon with the metal introduced into the arc in gaseous form (e.g., metal halide with high vapor pressure). Two previous experiments employing this method have been successful in determining *gf* values for nickel[3] and iron.[4] In both of these experiments, the metal tended to be concentrated preferentially in the lower-temperature zones of the arc. In the present experiment, most of the metal radiation is emitted from a visible ring concentric with the arc axis. This "demixing" effect makes side-on measurements impossible, and, thus, intensity measurements are taken end-on. The measurements are taken through one electrode with a small solid angle of observation, so that the observed radiation will come from a small volume of plasma over which the temperature is essentially constant, and there is no radiation coming from the ring where plasma conditions are quite different and the assumption of LTE is not valid.

EXPERIMENTAL PROCEDURE

The wall-stabilized arc is shown in Fig. 1. It is composed of six water-cooled copper disks (water passages not shown in figure), separated by Teflon rings which serve as electrical insulators and to seal the arc from the outside air. Since the disks are grooved to accept them, the Teflon gaskets are also used to align the pieces. The copper disks serve to constrict the arc to within a 4.8-mm-diameter channel, thus stabiliz-

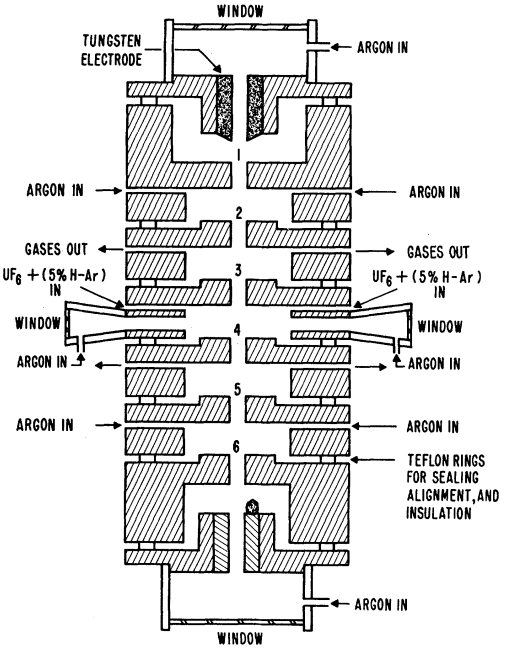

FIG. 1. Diagram of wall-stabilized arc.

ing the arc position and raising the axis temperature significantly. This elevated axis temperature was a disadvantage in that it ionized the uranium to such a degree that the U I line intensities were greatly reduced. In order to observe the U I lines in the wall-stabilized arc, the arc current would have to have been lowered to the point where the arc became unstable. The wall-stabilized arc was, however, quite adequate in the measurement of *gf* values of U II lines, and these supplied a means of temperature determination for the lower-temperature flow-stabilized arc, in which the U I lines could be observed.

The arc current is provided by a current-stabilized power supply, whose stability over several hours running time is about 0.2%. Most runs were made at a current of 25 A, which produced an arc axis temperature of approximately 10500 K. Argon flows into the arc tangentially at the points indicated in Fig. 1. A mixture of $Ar + H_2(5\%)$ flows into the central section at the rate of 500 ml/min. The hydrogen admixture is necessary for the temperature determination to be described below. Before entering the arc, the H_2-Ar mixture passes the mouth of a bottle filled with UF_6 crystals. The bottle is heated in a water bath to 70 °C which produces a UF_6 vapor pressure of ~2 atm. The amount of UF_6 vapor entering the H_2-Ar stream is controlled by a needle valve attached to the bottle. The valve is also immersed in the water bath to prevent clogging. The arc is equipped with windows for both side-on and end-on observation. Pure argon is streamed past the side windows, which are attached to the central section, in order to prevent them from being corroded by the UF_6. All gases are exhausted from the two sections adjacent to the central section, and pure argon flows into the two outer sections at the rate of 500 ml/min to each section. The flow arrangement is necessary in order that the uranium be confined to the central portion of the arc and kept away from the electrode region.

The flow-stabilized arc is shown in Fig. 2. Except for some small modifications, it is identical to the arc described by Richter.[2] The anode consists of a tungsten cup (threaded into a copper rod) on which a pellet of uranium is placed. The metal is put on the anode (instead of the cathode, as in the Richter arc) because this allows better evaporation of the uranium. Argon flows through a large nozzle around the anode to stabilize the arc. The flow is varied between 0.5 and 3 l/min and passes through a thick wire mesh, which distributes it uniformly before reaching the nozzle. It was found that the addition of N_2 to the stream also aided the evaporation of uranium. The cathode is a 6.4-mm tungsten rod, whose tip is situated in the bore of an insulated iron disk for stabilization of the arc. Both anode and cathode are insulated from the other parts of the mounting. A current of 5 A was adequate for stable running of the arc. As it evaporates from the anode, the uranium is drawn up into a mantle around the arc by thermal convection and from this mantle diffuses into the hot arc column. The arc is observed side-on through the mantle about 1 cm above the anode.

Both the wall- and flow-stabilized arc were observed with the same optical system which is shown in Fig. 3. The arc is imaged with a 2:1

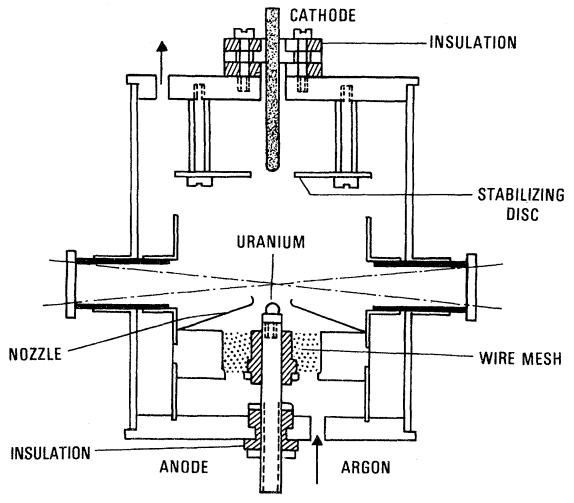

FIG. 2. Diagram of flow-stabilized arc.

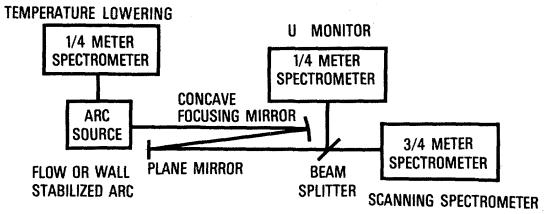

FIG. 3. Optical system.

enlargement onto the slits of a monitor and scanning monochromator using a concave mirror of 66-cm focal length and a beam splitter. All measurements of U II lines in the wall-stabilized arc were made end-on through a 3.2-mm hole in the cathode. A 12.7-mm diaphragm on the concave mirror limited the radiation to that coming from a very narrow cone ($f/80$) centered at the arc axis. To provide the necessary data needed to Abel invert the line intensities measured side-on and, hence, integrated over the cross section of the flow-stabilized arc, the concave mirror was motor driven, so that the image of the arc could be moved across the entrance slit of the scanning monochromator. A 1-in. diaphragm at the concave mirror limits the radiation to that coming from a small strip through the arc cross section, which is necessary in order that a sufficient number of points may be taken from the arc intensity profile and used in the Abel inversion process.

The spectral line intensities are measured photoelectrically with the amplified photomultiplier signal recorded on a strip chart. The instrument function of the scanning monochromator (20-μm slits) was 0.2 Å in first order and 0.1 Å in second order and was sufficiently larger than the widths of the uranium lines measured, so that the integrated intensities of the lines were proportional to the peak photomultiplier signal. Two 0.25-m monochromators are employed with reciprocal linear dispersion of 16 Å/mm in first order and fixed 25-μm slits. One monochromator is used to monitor a strong uranium line in order to account for small uranium concentration changes in the arc, and the other is used in the temperature determination of the wall-stabilized arc. A third monochromator of focal length 0.75 m with reciprocal linear dispersion of 11 Å/mm in first order was used to scan the lines of U I and U II. All lines above 4450 Å were measured in first order, while lower wavelengths were measured in second order since the line density is much greater in this wavelength region, and the better resolution is essential.

Because of the high density of lines in the spectrum, the background above which the signal height of a spectral line was measured could only be determined in a somewhat arbitrary way. It was chosen to be the lowest signal within 1 A on either side of the line.

To calibrate the line intensities measured from the arc on an absolute spectral radiance scale, the arc was removed and replaced by a tungsten strip lamp. Radiation from the arc and lamp thus passed through the same optical system. Any window that had been used in the arc was placed in the optical path when calibrating with the lamp. The spectral radiance of the tungsten strip lamp was previously determined with a blackbody by the Optical Radiation Section of the National Bureau of Standards.

For all runs with both the wall-stabilized arc and the flow-stabilized arc, the intensity of a strong uranium line (U I or U II, depending on which spectrum was being measured) was monitored, so that the measured intensities could be adjusted according to the change in the monitor produced by small changes in the uranium concentration. In addition, all lines for each run were measured relative to a given standard line, whose signal height was measured a number of times during the run and its variation checked with the monitor. The monitor signal for both arcs varied by no more than 30% for periods of up to 20 min. The short-term stability was much better as is illustrated in Fig. 4, which shows a wall-stabilized arc scan over a period of about 40 sec.

In order that relative oscillator strengths can be determined from measured relative line intensities, it is necessary that (a) the lines be optically thin, (b) the temperature be determined, and (c) the assumption of LTE be justified.

(a) The optical depth of uranium lines in the wall-stabilized arc was tested in the following manner. A good criterion for a line to be thin is that the line center is less than one-tenth of the blackbody function, i.e.,

$$(1/4\pi)P(\nu_U)[N_n A_{nm}]_U h\nu_U s_U < 0.1B(\nu_U, T)\,, \qquad (1)$$

where the subscript U refers to uranium, ν_U is the central frequency of the uranium line, s_U is the length of plasma emitting the uranium line, P

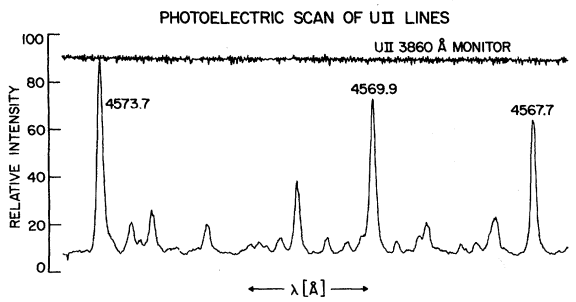

FIG. 4. Photoelectric scan of U II lines and monitor from wall-stabilized arc.

is the line-shape function, N_n the number of atoms in the upper state, and A_{nm} is the transition probability. The intensity ratio of an argon line and a uranium line is given by

$$\frac{I_{Ar}}{I_U} = \frac{[N_n A_{nm}]_{Ar} s_{Ar} h\nu_{Ar}}{[N_n A_{nm}]_U s_U h\nu_U} . \quad (2)$$

Solving for s_U in Eq. (1) and substituting in Eq. (2), expressing quantities in terms of λ, and substituting the Doppler expression for the line-shape function at the line center, the following inequality results:

$$\frac{I_{Ar}}{I_U} > \frac{5 s_{Ar}}{2\pi} \frac{[A_{nm}N_n]_{Ar}}{B(\lambda_U, T)} \left(\frac{Mc^2}{2\pi k T \lambda_U^2}\right)^{1/2} , \quad (3)$$

where M is the mass of the uranium atom, and the quantity s_{Ar} is just the length of the arc channel since the arc is essentially burning in pure argon, except for the introduction of UF_6 in the central section. The relation is over-restrictive to the extent that, while pressure broadening is present and will lower the peak height of the uranium line, only Doppler broadening has been considered in this derivation. Use of the above relation involves only relative intensity and temperature measurements, but the absolute transition probability A_{nm} must be known for the argon line, whose intensity is measured relative to that of the uranium line. A number of runs were made with the above criterion fulfilled for the strongest U II line (3859.6 Å) measured. When the uranium concentration was increased by adding more UF_6, it was found that no change in intensity ratios resulted for temperature insensitive lines of approximately the same upper energy level. The concentration could not be increased very much before the ring of demixed uranium became distorted and closed into the center of the arc, making axis measurements meaningless. Hence, for all feasible running conditions, it could be safely assumed that the U II lines were optically thin.

For the flow-stabilized arc, a strong U II line was used for the temperature determination; therefore, an optical depth check was made using the intensity ratio of the strong 3859.6-Å U II line and a weaker line of the same upper energy level. The ratio was the same as that observed in the wall-stabilized arc. When N_2 was added to the gas flow around the anode, more uranium was evaporated into the arc column, and the ratio changed, indicating that self-absorption in the strong line was starting to take place. In order to bring the U I lines up to a measurable intensity, it was necessary to have some N_2 in the gas flow, but the amount was always kept below that which would cause the 3859.6-Å line to become optically thick. The U I lines measured were all weaker than the 3859.6-Å line by an order of magnitude and, consequently, were optically thin.

(b) The temperature of the wall-stabilized arc is determined in the following manner. The arc is initially operated with only the $Ar + H_2$ (5%) mixture (without UF_6) flowing into the central section. The hydrogen admixture allowed measurement of the Balmer H_β line profile, whose halfwidth is a sensitive function of electron density. The electron density is calculated from the halfwidth using theoretical Stark broadening calculations[5] with an empirical correction according to Wiese *et al.*[6] Use of the Saha equation and the ideal gas law allows the calculation of the temperature from the electron density, assuming a constant-pressure (1 atm) arc. The H_β measurement is made end-on through the electrodes, and, simultaneously, the side-on intensity of a strong Ar I line is recorded. As the UF_6 is introduced into the central arc section, the intensity of the argon line is seen to decrease implying a decrease in temperature which is calculated from the temperature dependence of the argon line. Concerning the determination of the temperature lowering, it must be established that the decrease in intensity of the Ar I line measured side-on is not due simply to displacement of argon by the introduction of UF_6. Measurement of a strong fluorine line end-on demonstrated that displacement of argon by fluorine was negligible. Since the stoichiometric ratio of fluorine to uranium is 6, one would, consequently, expect the displacement effect by the uranium to be negligible. However, owing to the demixing effect, the uranium concentration becomes very high in a ring about the arc axis. This ring has a relatively large diameter which was measured to be about 3 mm. End-on scans of the Ar I line revealed that the major portion of its radiation was coming from atoms well within the region of the ring.

The data analysis of the flow-stabilized arc is more involved to the extent that measurements were taken side-on. The temperature measurement (employing U II gf values measured in the wall-stabilized arc) and the relative gf values of the U I lines measured were obtained from local emission coefficients $\epsilon(r)$ which came from the Abel inversion of side-on intensity scans $I(y)$, i.e.,

$$\epsilon(r) = -\frac{1}{\pi} \int_r^{r_0} \frac{[dI(y)/dy]dy}{(y^2 - r^2)^{1/2}} . \quad (4)$$

The $I(y)$ are obtained from strip chart recordings of the photomultiplier signal as the image of the arc is moved across the entrance slit of the spectrometer by the motor-driven concave mirror. r_0 is the radius beyond which the emission is neg-

ligible. The inversion of this data is based on a curve-fitting technique[9,10] in which the data are integrated numerically to find the coefficients of orthogonal Legendre polynomials which are used in Eq. (4) to evaluate $\epsilon(r)$.

For an efficient data analysis, it is advantageous to use the complex Abel inversion procedure only on a few selected lines of different upper state energy and apply to the rest of the lines the following greatly simplified analysis, which involves the introduction of an "equivalent path length." One measures the side-on intensities $I(0)$ integrated over the maximum arc cross section. The equivalent path length $s(r, E)$ is then defined as follows:

$$s(r, E) = I(0)/\epsilon(r, E) , \tag{5}$$

where

$$\epsilon(r, E_n) = \frac{hc}{4\pi\lambda} N_n(r) A_{nm} = \frac{2\pi e^2 h}{m} \frac{g_m f_{mn}}{\lambda^3} \frac{N_0(r)}{Z} e^{-E_n/kT(r)} . \tag{6}$$

Combining Eqs. (5) and (6), one can write an expression for the relative intensities:

$$\frac{I_1(0)}{I_2(2)} = \frac{gf_1}{gf_2} \frac{\lambda_2^3}{\lambda_1^3} \frac{s(r, E_1)}{s(r, E_2)} \exp\left(-\frac{(E_1 - E_2)}{kT(r)}\right) . \tag{7}$$

Seven U I lines of various upper-state energies were selected for the Abel inversion process and yielded equivalent path lengths for the respective energies according to Eq. (5), and from these, path lengths for all other lines were interpolated. Using these path lengths, relative U I gf values were then calculated using Eq. (7) with the temperature from the relative intensity of two U II lines (which were Abel inverted) and the intensities $I(0)$ of the U I lines integrated over the maximum arc cross section. For this analysis, the radial position $r = 2.7$ mm was chosen, where the information coming from both U I and U II is relatively reliable. The data were not analyzed at smaller radial distances since the behavior of the emission coefficient versus radius for the U I lines indicates that there is much U I emission from the outer portions of the arc, and, hence, results from the Abel inversion for points near the arc axis become unreliable. The situation is almost reversed for the U II line of higher upper-state energy used in the temperature determination. Information from points near the axis is more reliable, and temperatures calculated from points too far from the axis carry greater uncertainties.

(c) A useful theoretical criterion as to whether the assumption of LTE is valid is the following expression[11]:

$$N_e \geq 1.6 \times 10^{12} T^{1/2} \Delta E^3 , \tag{8}$$

where ΔE is in eV. If this is fulfilled for the largest energy gap in the energy level schemes of the atom and the ion, then both the Saha equation and the Boltzmann distributions are valid, and the plasma is in complete LTE. If it is sufficient to have a Boltzmann distribution for the higher excited states only, then the energy term in Eq. (8) is the much smaller energy separation between the high levels. Such "partial" LTE is achieved at much lower values of N_e. Using known energy levels of U II (Ref. 12) and the temperature of the wall-stabilized arc, the criterion expressed by Eq. (8) yields $N_e \geq 5.8 \times 10^{10}$ cm^{-3} as the limiting electron density above which partial LTE should exist. Typical wall-stabilized and flow-stabilized arc electron densities in this experiment were 3×10^{16} and 5×10^{13} cm^{-3}, respectively. The measurement of U I gf values relative to those of U II in the wall-stabilized arc (see below) requires complete LTE for uranium. For this case, Eq. (8) requires $N_e \geq 1.0 \times 10^{13}$ cm^{-3} which is still well below the measured electron density of the wall-stabilized arc.

In addition to these theoretical estimates, an experimental check was made on the equilibrium of the levels of U II using gf-value measurements from the wall-stabilized arc. The results are given in Table I which shows the gf-value ratio of the 2941.9-Å line (upper-state energy of 39 508 cm^{-1}) to the 5493.0-Å line (upper-state energy of 18 200 cm^{-1}). A change in the ratio (outside of experimental error) as a function of electron density would indicate departures from partial LTE. A similar check is provided by comparing gf values of U II measured in the wall-stabilized arc and in the flow-stabilized arc since the two sources have electron densities which differ by a factor of about 600. Although the flow-stabilized arc was used primarily for the measurement of U I lines, a run was made where a number of U II lines were measured for comparison with wall-stabilized arc results. The comparison is shown in Fig. 5. A departure of the points from a horizontal line as a function of upper-state energy would indicate departures from partial LTE.

In the initial (before UF_6 is added) temperature determination of the wall-stabilized arc, the argon

TABLE I. gf_{2942}/gf_{5493} for different electron densities.

Ratio	N_e (10^{16} cm^{-3})
26.2	0.88
27.4	1.65
24.4	2.47
27.9	3.42
24.4	4.00

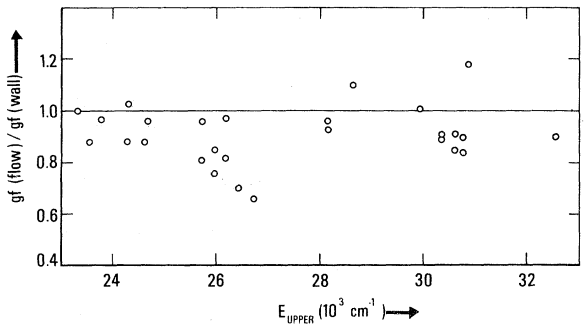

FIG. 5. Ratio of flow-stabilized arc gf values to wall-stabilized arc gf values vs upper-state energy.

was assumed to be in complete LTE in order that the Saha equation could be used in calculating the temperature from the electron density. Equation (8) yields $N_e \geq 2.5\times10^{17}$ cm^{-3} for the typical wall-stabilized arc temperature of 10500 K. Recent experimental studies[7] have shown that argon is in complete LTE only for electron densities above 5×10^{16} cm^{-3}. Since the electron densities in the wall-stabilized arc were typically about 3×10^{16} cm^{-3}, it was necessary to check for the size of any departures from LTE. The determination of the electron density from the width of the H_β line does not depend sensitively on the existence of LTE. Another determination of the electron density, which is dependent upon Saha equilibrium, was made for comparison. The absolute intensity of the 4300.1-Å Ar I line was measured, and line wing corrections[8] were made to ensure that the total intensity of the line was obtained. Using the measured intensity of the argon line, the Saha equation, and the ideal gas law, the three unknowns T, N_e, and the density of neutral argon were obtained. The resultant electron density was compared with that determined from the H_β measurement, and the difference was within the error of measurement (i.e., the error in N_e resulting from the H_β width measurement was estimated at 10%). Since a 10% error in N_e reflects a temperature error of 1.5%, any errors in temperature larger than this due to departures from LTE were ruled out.

The preceding discussion relates to relative gf values within the same stage of ionization. In order to put the U I and U II relative gf values on the same scale, it is necessary to measure the intensity of a U I line relative to a U II line. This appeared to be possible in the wall-stabilized arc since a number of the strongest U I lines were present, although very weak. On closer inspection, it was found that all the U I lines identified, except the 3812.0-Å line, were blended with U II lines and could not be measured reliably. A measurement was made of the intensity of the 3812.0-Å line relative to the 3826.5 U II line, and by use of the Saha equation for uranium, the relative gf ratio for these two lines was calculated. The result was uncertain by about 50%, owing mainly to the uncertainty in the continuous background which had to be subtracted from the 3812.0-Å line intensity. Since the dependence on partition functions in the calculation cancels out, the unreliable value of the partition function for U II (due to sparsely classified energy levels) did not contribute to the final uncertainty.

RESULTS AND DISCUSSION

The results of the experiment are shown in Tables II and III. Table II contains absolute gf values for 22 lines of U I. The scale has been obtained by adjusting the gf values of the 3584.9-Å and the 4620.2-Å lines (while maintaining their measured relative values) so that they agree with the recently measured lifetime[13] of $\tau = 7.3$ nsec for the 27 887-cm^{-1} level of U I. This normalization is possible because all other transitions from this level are negligibly weak. Table III contains absolute gf values for 49 lines of U II. The U II absolute scale has been obtained by adjusting the gf value of the 3826.5 U II line relative to the gf value of the 3812.0 U I line, so that the ratio agrees with the measurement made in the wall-stabilized arc. For comparison, the data from

TABLE II. U I gf values.

Wavelength (Å)	Lower energy (cm^{-1})	Upper energy (cm^{-1})	gf_{expt}	$gf_{Corliss}$
3584.9	0	27 887	2.4	2.1
3812.0	0	26 226	0.71	1.7
3839.6	3801	29 838	1.9	3.1
3854.2	0	25 938	0.55	0.53
3871.0	0	25 826	0.85	1.2
3894.1	0	25 672	0.43	0.40
3943.8	0	25 349	0.99	0.94
4005.2	620	25 580	0.32	1.1
4005.7	620	25 577	0.23	
4047.6	620	25 319	0.46	0.34
4154.0	0	24 067	0.69	0.55
4222.4	3801	27 478	0.92	0.61
4246.3	0	23 544	0.40	0.15
4362.1	0	22 919	0.74	0.23
4393.6	0	22 754	0.60	0.17
4426.9	0	22 583	0.14	0.034
4516.7	620	22 754	0.25	0.038
4620.2	6249	27 887	2.6	0.76
4631.6	0	21 585	0.45	0.10
4790.1	3801	24 671	0.17	0.054
5027.4	0	19 885	0.53	0.070
5164.1	8119	27 478	0.72	0.21

NBS Monograph 53, [14] which contains the only other measurements of uranium *gf* values, are listed in both tables.

On a relative scale, errors in the final values arise from three principal sources:

(a) Deviations in the measured intensities from run to run. One of the major reasons for these deviations in the wall-stabilized arc was radiation from the ring of demixed uranium. For small concentrations of uranium, the ring was well defined, but measurements were difficult because of the small line-to-continuum ratio. For larger concentrations, the ring became distorted, and although the greatest effort was made to eliminate it, there always existed the possibility that radiation from the ring was reaching the monitor monochromator and not the scanning monochromator or vice versa. In the flow-stabilized arc, the addition of a small amount of nitrogen to the gas flow around the anode allowed stronger U I emission. The nitrogen had an adverse effect on the stability of the arc, and this was undoubtedly part of the cause for varying results from run to run. The standard deviation of the mean was calculated for the number of measurements of each line.

(b) Uncertainty in the tungsten strip lamp calibration. This error was estimated not to exceed 2% for all wavelengths measured in the experiment.

(c) Error in the temperature measurement. For the wall-stabilized arc, the error in the initial temperature determination before UF_6 was added was estimated at 3%. This figure takes into account errors in the H_β width measurement and uncertainties in the width data from which the electron density was calculated. The error in the temperature lowering due to the addition of uranium was estimated at 40%. This error was due principally to the uneven density distribution of uranium along the axis (i.e., the temperature lowering is large at the central arc section where the argon line is observed, but goes to zero toward the outermost sections of the arc as the uranium diffuses out of the arc column). Since the 40% error occurs for a temperature lowering which was typically 400 K, this amounts to an error in the final temperature of 1.5%. The error in determining the flow-stabilized arc temperature was obtained by considering the uncertainty in the relative *gf* values (measured in the wall-stabilized arc) of the U II lines used to determine the temperature and the error in measuring their relative intensity. The total temperature error was estimated at 5%. The temperature error for both arcs must be multiplied by the term $\Delta E/kT$ to give the error in relative *gf* values. The term

TABLE III. U II *gf* values.

Wavelength (Å)	Lower energy (cm^{-1})	Upper energy (cm^{-1})	gf_{expt}	$gf_{Corliss}$
2941.9	5527	39508	0.66	1.7
3111.6	1749	33877	0.19	0.29
3305.9	2294	30240	0.12	0.14
3550.8	0	28154	0.052	0.10
3670.1	915	28154	0.26	0.38
3700.6	915	27930	0.046	0.092
3701.5	5527	32535	0.24	0.68
3746.4	5527	32211	0.10	0.40
3748.7	5716	32384	0.23	0.56
3782.8	289	26717	0.088	0.25
3826.5	289	26415	0.041	0.092
3831.5	4663	30756	0.20	0.84
3854.7	4663	30599	0.26	0.98
3859.6	289	26191	0.24	0.58
3865.9	2295	28154	0.14	0.39
3881.5	4585	30342	0.10	0.39
3890.4	289	25986	0.10	0.25
3932.0	289	25714	0.15	0.22
3985.8	5260	30342	0.19	0.48
3992.5	5716	30756	0.074	0.18
4017.7	5716	30599	0.11	0.26
4050.0	0	24684	0.078	0.15
4051.9	5260	29932	0.12	0.21
4062.6	0	24608	0.075	0.078
4067.8	6283	30860	0.093	0.27
4090.1	1749	26191	0.20	0.31
4116.1	0	24288	0.064	0.068
4124.7	1749	25986	0.055	0.055
4128.3	4420	28636	0.071	0.12
4141.2	8394	32535	0.20	0.40
4171.6	1749	25714	0.11	0.18
4241.7	4585	28154	0.21	0.28
4244.4	0	23554	0.052	0.039
4341.7	289	23315	0.061	0.051
4372.6	915	23778	0.029	0.014
4373.4	1749	24608	0.024	0.012
4472.3	289	22642	0.066	0.040
4515.3	289	22429	0.029	0.016
4538.2	1749	23778	0.028	0.018
4543.6	915	22917	0.069	0.048
4567.7	1749	23635	0.023	0.0090
4569.9	289	22165	0.021	0.0085
4571.0	6283	28154	0.023	0.014
4573.7	2295	24152	0.033	0.018
4641.7	8399	29932	0.037	0.040
4689.1	0	21320	0.021	0.010
4722.7	1749	22917	0.028	0.015
4731.6	4585	25714	0.033	0.026
5493.0	0	18200	0.025	0.0068

TABLE IV. Intensities derived at 5100 °K using gf values from Ref. 14 and this experiment.

λ	Above 4300 Å Ref. 14	This work	λ	Below 4050 Å Ref. 14	This work
		Lines above 20 in intensity			
4341.7	50	23	4050.0	120	25
			3932.0	150	40
4472.3	44	28	3890.4	160	25
			3859.6	360	59
4543.6	46	26	3670.1	160	42
		Lines below 10 in intensity			
4372.6	12	9.6	4017.7	42	7.1
4373.4	8	6.4	3992.5	28	4.4
4538.2	14	8.1	3881.5	75	7.8
4567.7	7	6.9	3826.5	55	9.6
4569.9	10	9.7	3746.4	50	4.9
4571.0	3	1.9	3701.5	40	7.7
4573.7	12	8.3	3550.8	48	9.3
4641.7	5	1.8	3111.6	40	9.7
4722.7	13	9.2	2941.9	55	8.4
4731.6	10	7.4			

ΔE varies from line to line according to the difference between the upper-state energy of the measured line and that of the standard line with respect to which all the lines were measured. Possible errors arising from other sources, such as the Abel inversion process, instabilities in the amplifiers and photomultipliers, etc., were estimated to be negligible compared with the errors discussed above. The errors described in (a)–(c) were treated as independent and combined as follows:

$$\frac{\Delta gf}{gf}=\left[\left(\frac{\Delta I}{I}\right)^2+\left(\frac{\Delta I_{\text{lamp}}}{I_{\text{lamp}}}\right)^2+\left(\frac{\Delta E}{kT}\,\frac{\Delta T}{T}\right)^2\right]^{1/2}. \qquad (9)$$

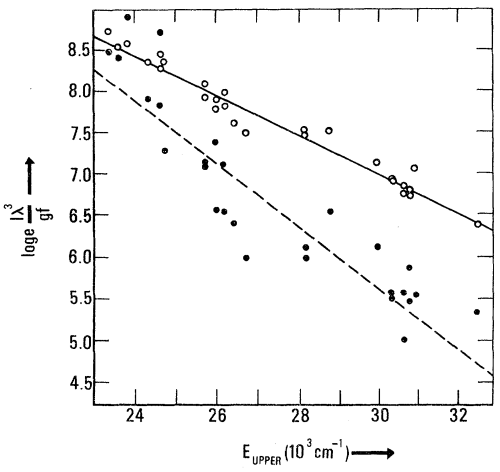

FIG. 6. $\ln(I\lambda^3/gf)$ vs upper-state energy using flow-stabilized arc intensities for U II lines. The dots represent values calculated from Ref. 14 gf values. The open circles represent values calculated from gf values measured in the wall-stabilized arc.

On a relative scale, the errors for both U I and U II ranged between 5% and 10%.

On an absolute scale, three additional errors must be considered which are the error in the lifetime measurement (<15%),[13] the error (due to the error in the temperature) in applying the Saha equation to put the U I and U II gf values on the same scale (<20%), and the error in subtracting the background from the U I 3812.0 line (<50%). These errors, when added to the errors in the relative values, result in a total error of 20% for the U I gf values and 60% for the U II gf values.

As mentioned previously, the only other measurements of uranium are contained in NBS Monograph 53 (Ref. 14). The measurements were made employing a free-burning arc run at 10 A dc. There was a small amount of uranium added to the copper electrodes. The temperature and electron density were 5100 K and 2.4×10^{14} cm^{-3}, respectively, and the measurements were made photographically, side-on, and with no Abel inversion.

Looking at the comparison of results for U II in Table III, it is seen that on a relative scale the measurements agree fairly well, except that there appears to be a wavelength-dependent factor which takes the Monograph 53 values from about 0.6 times the present values above 4300 Å to approximately a factor of 3 times the present values below 4000 Å. At first, it was thought that this discrepancy might be intensity rather than wavelength dependent. Intensities were calculated from both sets of gf values for $T=5100$ °K. The calculated Monograph 53 intensities were normalized to 120 for the 4050.0-Å line, whereas the intensities calculated from this experiment were normalized to

25. Table IV presents the results arranged according to wavelength region and intensity and shows that the discrepancies are wavelength rather than intensity dependent.

An over-all comparison of the two sets of *gf* values is provided by Fig. 6. A run was made with the flow-stabilized arc in the wavelength region 3750–4400 Å, and a number of U II relative line intensities were measured. Instead of performing the Abel inversion for each line intensity measurement, the equivalent path lengths for selected U II lines were plotted, and the correction factors for other lines were interpolated from the graph as was done with the U I line analysis. The corrected intensities were used to calculate the quantity $\ln(I\lambda^3/gf)$ employing the *gf* values of Monograph 53 and of this experiment, and the results were plotted against upper-state energy. The plot shows the over-all consistency of the *gf* values measured in the wall-stabilized arc with the flow-stabilized arc intensities and also demonstrates the large scatter of the Monograph 53 values. The dashed line drawn through the points calculated from the Monograph 53 data corresponds to a temperature of about 3800 °K, which is unrealistic for the flow-stabilized arc.

The comparison for U I appears in Table II. The wavelength effect is quite noticeable here also. The neglect of Abel inversion in obtaining the Monograph 53 data should not have any appreciable effect in the case of the U I lines considered since the spread in upper energy levels is relatively small. The same can be said for most of the U II lines. The principal reason for discrepancies between the Monograph 53 data and this work seems to be the use of photographic rather than photoelectric techniques.

The measurement of *gf* values in two sources that have significantly different temperatures and electron densities, as realized in this experiment for the U II lines, reduces the chance of systematic errors. Because of the large line-to-continuum ratio of U II lines in the flow-stabilized arc, the measurement of a great many more U II lines is possible in this arc, using U II lines already measured in the wall-stabilized arc for a temperature determination.

---

*Research supported in part by the advanced Research Projects Agency of the Department of Defense under the Strategic Technology Office.

[1]D. W. Steinhaus, M. V. Phillips, J. B. Moody, L. J. Radziemski, K. J. Fisher, and D. R. Hahn, Report LA-4944, Los Alamos Sci. Lab., 1972 (unpublished).

[2]J. Richter and P. Wulff, Astron. Astrophys. 9, 37 (1970).

[3]G. D. Bell, D. R. Paquette, and W. L. Wiese, Astrophys. J. 143, 559 (1966).

[4]J. M. Bridges and W. L. Wiese, Astrophys. J. 161, L71 (1970).

[5]P. Kepple and H. R. Griem, Phys. Rev. 173, 317 (1968).

[6]W. L. Wiese, D. E. Kelleher, and D. R. Paquette, Phys. Rev. A 6, 1132 (1972).

[7]J. B. Shumaker and J. Popenoe, J. Res. Natl. Bur. Stand. (U. S.) A 76, 71 (1972).

[8]W. L. Wiese, in *Plasma Diagnostic Techniques*, edited by R. H. Huddlestone and S. L. Leonard (Academic, New York, 1965), Chap. 5.

[9]M. P. Freeman and S. Katz, J. Opt. Soc. Am. 53, 1172 (1963).

[10]C. H. Popenoe and J. B. Shumaker, J. Res. Natl. Bur. Stand. (U. S.) A 69, 495 (1965).

[11]R. W. P. McWhirter, in Ref. 8, Chap. 5.

[12]D. W. Steinhaus, L. J. Radziemski, R. D. Cowan, J. Blaise, G. Gvelachvili, B. O. Zëineb, and J. Vergés, Report LA-4501, Los Alamos Sci. Lab., 1971 (unpublished).

[13]J. Z. Klose, preceding paper, Phys. Rev. A 11, 1840 (1975).

[14]C. H. Corliss and W. R. Bozman, Natl. Bur. Stand. (U. S.), Monogr. 53 (1962).